



Bone bonding ability of some borate bio-glasses and their corresponding glass-ceramic derivatives

Fatma H. Margha^{1,*}, Amr M. Abdelghany²

¹Glass Research Department, National Research Center, Cairo, 12311, Egypt

²Spectroscopy Department, Physics Division, National Research Center, Cairo, 12311, Egypt

Received 27 May 2012; received in revised form 1 September 2012; accepted 3 November 2012

Abstract

Ternary borate glasses from the system $\text{Na}_2\text{O}\cdot\text{CaO}\cdot\text{B}_2\text{O}_3$ together with soda-lime-borate samples containing 5 wt.% of MgO , Al_2O_3 , SiO_2 or P_2O_5 were prepared. The obtained glasses were converted to their glass-ceramic derivatives by controlled heat treatment. X-ray diffraction was employed to investigate the separated crystalline phases in glass-ceramics after heat treatment of the glassy samples. The glasses and corresponding glass-ceramics after immersion in water or diluted phosphate solution for extended times were characterized by the grain method (adopted by several authors and recommended by ASTM) and Fourier-transform infrared spectra to justify the formation of hydroxyapatite as an indication of the bone bonding ability. The influence of glass composition on bioactivity potential was discussed too.

Keywords: glass, glass-ceramics, FTIR spectroscopy, corrosion, bioactivity

I. Introduction

The first patented bioactive glass 45S5 was first reported by Hench in 1971 [1], and its composition was a modified soda-lime-silica with addition of P_2O_5 . The successful application of this first bioglass [2] together with Cera Vital® bioactive glass-ceramics [3], A-W glass ceramic [4], dense hydroxyapatite ceramic [5] and other materials in clinical applications [6] have stimulated research in the development of bioactive glasses and bioactive glass-ceramics with improved properties. Bioactive glasses and glass-ceramics are known to bond to living bones in the body through formation of hydroxyapatite (HCA) layer on their surfaces [2,7,8]. Most of the published works on bioactive glasses and glass-ceramics have been concentrated on SiO_2 -based or P_2O_5 -based materials [2,8–13]. Bioactive glasses containing B_2O_3 in their compositions have been mentioned in some researches [2,14,15]. Hench mentioned in his review on bioceramics a patented bioglass containing 15 wt.% B_2O_3 [1,2] and it was designated as (45B15S5). Osaka *et al.* [14] have examined the bioactivity of calcium and sodium borosilicate glasses by

immersion in simulated body fluid. The superior bioactivity of the calcium glasses in comparison to the sodium glasses was attributed to the existence of calcium ions in the vicinity of silanol groups in hydrated silica gel formed in the fluid. The best bioactivity of $30\text{Na}_2\text{O}\cdot 20\text{B}_2\text{O}_3\cdot 50\text{SiO}_2$ among the sodium glasses was attributed to the presence of the largest fraction of Si atoms bonding to two bridging oxygen atoms.

EI Batal and EI Khesheh [15] have prepared and characterized some substituted glasses based on Hench's patented bioglass®. They showed that the introduction of 10 wt.% of B_2O_3 replacing SiO_2 increases the corrosion of the glasses by various leaching solutions and reaches 30% after 1 hour at 90 °C in 0.1N HCl solution (determined by the grain method).

Pure borate glasses have only recently been explored for use in biomedical applications. Richard was the first who investigated replacing SiO_2 completely with B_2O_3 in the 45S5 glass composition [16]. The borate based 45S5 immersed in a K_2HPO_4 solution at body temperature (37 °C) formed a layer of hydroxyapatite (HA), $\text{Ca}_{10}(\text{PO}_4)_6(\text{OH})_2$, similar to that formed by the Hench's silicate based 45S5. The in vitro formation of HA from the borate based 45S5 led to further investigation in vivo. Particles of the borate based 45S5 glass

* Corresponding author: tel: +202 33371362
fax: +202 33387803, e-mail: fatmamargha@yahoo.com

were placed in a rat tibial defect, and not only promoted bone formation, but did so at a faster rate than the silicate based 45S5 glass.

Huang *et al.* [17,18] have described and compared the reaction mechanisms for both the silicate 45S5 glass and the borate analogue of 45S5 glass. The borate glass is fully converted to HA by the glass dissolving, (B_2O_3 and Na_2O are dissolved into solution, and the CaO is reacting with PO_4^{3-} from the phosphate solution). On the other hand, the silicate glass is partially converted to HA, while leaving a sodium depleted core surrounded by a silica-rich layer.

Jung and Day [19] have carried out a kinetic analysis of the reaction rate of the conversion kinetics of silicate, borosilicate and borate bioactive glasses to hydroxyapatite. The reaction rate increased with increasing the B_2O_3 content, and the borate glass reacted almost five times faster than the analogous silicate glass. The change or deviation from the suggested contracting volume model for borate glass to the slower 3D diffusion model is attributed to the formation of a silica-rich layer of a certain thickness that began controlling the release of ions from the unreacted glass by diffusion. The borate bioglass is completely dissolved and converted to hydroxyapatite.

The main objective of this work is to determine the corrosion weight loss of some prepared ternary soda-lime-borate glasses and some derived samples containing substituted 5 wt.% of Al_2O_3 , SiO_2 , MgO or P_2O_5 by

the use of sodium phosphate (Na_2HPO_4) solution or distilled water for comparison with the recommended grain method. Also, the study includes the investigation of the FTIR spectra of the prepared glasses before and after immersion to follow the formation of hydroxyapatite. The work also includes the preparation of glass-ceramic derivatives through controlled heat treatment of the parent borate glasses. The same corrosion and Fourier-transform infrared investigations were repeated on the crystalline derivatives aiming to follow the potential bioactivity of both glassy and crystalline derivatives.

II. Experimental

2.1 Preparation of glasses and glass-ceramics

The glasses were prepared from chemically pure grade materials with the composition shown in Table 1. The materials include H_3BO_3 for B_2O_3 , whereas Na_2O , CaO and MgO were introduced in the form of their respective carbonates. Al_2O_3 was added in the form of calcined pure Al_2O_3 while P_2O_5 was added in the form of ammonium dihydrogen phosphate ($NH_4H_2PO_4$), and pure calcined quartz for the introduction of SiO_2 .

The weighed batches were melted in platinum crucibles at 1050 °C for 2 hours. The melts were rotated at intervals of 30 minutes apart. The homogenized melts were cast into warmed stainless steel moulds of the required dimensions. The prepared samples were immediately transferred to a muffle furnace regulated at

Table 1. Chemical composition of the studied glasses

Glass No.	Composition [wt.%]						
	Na_2O	CaO	B_2O_3	MgO	Al_2O_3	SiO_2	P_2O_5
G1	20	20	60	-	-	-	-
G2	15	15	70	-	-	-	-
G1-Mg	20	20	55	5	-	-	-
G1-Al	20	20	55	-	5	-	-
G1-Si	20	20	55	-	-	5	-
G1-P	20	20	55	-	-	-	5

Table 2. DTA parameters and corrosion weight loss

Glass No.	Thermal treatment		Weight loss [wt.%]	
	nucleation	crystal growth	in H_2O	in Na_2HPO_4 solution
G1			10.0	28.0
GC1	450 °C/5 h	650 °C/6 h	14.28	32.43
G2			15.78	31.5
GC2	450 °C/5 h	650 °C/6 h	23.53	51.28
G1-Mg			12.0	3.85
GC1-Mg	450 °C/5 h	650 °C/6 h	6.97	8.16
G1-Al			16.6	15.1
GC1-Al	450 °C/5 h	650 °C/6 h	16.66	18.9
G1-Si			17.14	24.0
GC1-Si	450 °C/5 h	650 °C/6 h	13.04	30.7
G1-P			23.5	34.6
GC1-P	450 °C/5 h	650 °C/6 h	17.24	35.7

380 °C for annealing. The muffle was switched off after 1 hour and left to cool down to room temperature at a rate of 25 °C/h.

The glass samples were thermally heated in a two-step regime (Table 2). Thus, each glass was heated slowly to 450 °C with holding time of 5 hours to form of sufficient nuclei sites and then further heated to reach the second chosen crystal growth temperature at 650 °C. After holding time of 6 hours the specimens were left to cool inside the muffle to room temperature at a rate of 20 °C/hour.

2.2 Sample characterization

Differential thermal analysis (DTA) was carried out on powdered glass samples which were examined up to 1000 °C using powdered alumina as a reference material. DTA Perkin Elmer DTA-7 apparatus was used to find out the proper heat treatment temperatures to obtain appropriate glass-ceramic derivatives with high crystallinity. Briefly, the values obtained for glass nucleation temperatures and the onset of crystallization temperatures are given in Table 2.

The heat treated glass-ceramic specimens were analysed by X-ray diffraction in order to identify the crystalline phases that precipitated within these crystalline samples during the heat treatment and conversion to glass-ceramic derivatives. The glass-ceramic samples were ground and the fine powder was examined using a diffractometer with a Ni-filter and Cu-target. The X-ray diffraction patterns were obtained using a Phillips PW 1390 X-ray diffractometer. The diffraction patterns were identified with comparison with standard ASTM cards and published data of similar compositions.

The chemical corrosion of the prepared bioglasses and their corresponding glass-ceramics derivatives was carried out using the grain method which was adopted by several authors [15,20–24] and recommended by ASTM specifications. Glass grains (0.30–0.60 mm in diameter) were immersed in distilled water and disodium hydrogen phosphate (Na_2HPO_4) solution (0.25 M) for 1 hour at 90 °C. In both cases 1 g of sample grains was placed in a sintered glass crucible G4 (Jena type) which was placed in a 250 ml polyethylene beaker situated in the water bath regulated at 90 °C. 150 ml of the attacking solutions was introduced to cover the grains. After 1 hour, the beaker was removed from the bath and the sintered glass crucible was fitted onto a suction pump and the whole solution was pumped through it. The sintered glass crucible was transferred to an air oven at 120 °C for 1 hour. Then, the cooled crucible with its content was reweighed and the total loss was calculated. An empty sintered glass crucible of the same type (G4 Jena) was subjected to the same corrosion test and the obtained result was taken into consideration.

Infrared absorption spectra of the bioglasses and their glass-ceramic derivatives were measured at room

temperature (~ 20 °C) in the wavenumber range 4000–400 cm^{-1} using a Fourier-transform infrared spectrometer (type Jasco FT-IR, Japan). Fine powders of the samples were mixed with KBr in the ratio 1:100 and the mixtures were subjected to a load of 5 tons/ cm^2 in an evacuable die to produce clear homogeneous discs. Then, the IR absorption spectra were measured immediately after preparing the discs to avoid moisture attack. The same FTIR measurements were repeated after immersion of the glasses and crystalline glass-ceramic derivatives in sodium phosphate solution for prolonged time (30 days) or distilled water.

UV-visible absorption spectra of polished samples of the dimensions $4 \times 1 \times 0.2$ cm were recorded to confirm their homogeneity and high transmittance, especially in the visible region. A recording spectrophotometer type T 80, PG Instruments, England, was utilized within the wavelength range 200–1000 nm.

III. Results and discussion

3.1 Optical absorption spectra

Figure 1 shows that all the studied soda-lime-borate glasses exhibit strong ultraviolet absorption spectra, but without absorption bands in visible region indicating their uniformity and clearness within this region. The spectrum of the glass G1 shows strong and wide UV absorption extending from 200–330 nm, revealing four successive peaks at about 210, 235, 260 and 285 nm decreasing in intensity with larger wavelengths while no bands could be identified in the visible region.

The glass G2 reveals similar spectral characteristics, only the fourth peak at 285 nm disappears with the increase of B_2O_3 (or with the decrease of the modifier contents). On the other hand, the ultraviolet absorption peaks of the glasses with smaller amount of B_2O_3 and presence of different modifier (samples G1-Mg, G1-Al, G1-P, and G1-Si) are less pronounced. Cook and Mad-

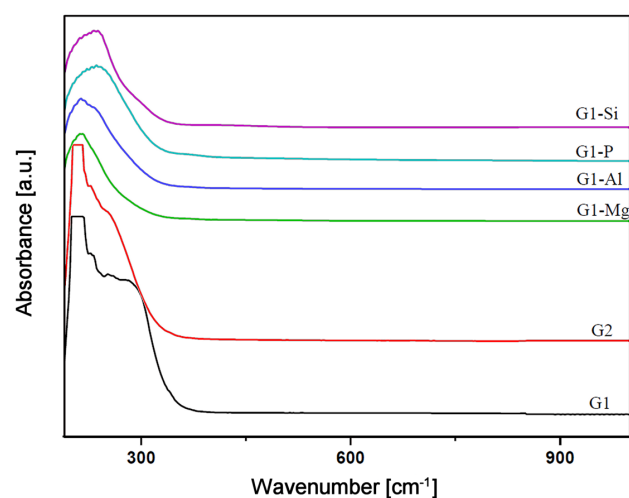


Figure 1 UV-visible absorption spectra of the studied glasses

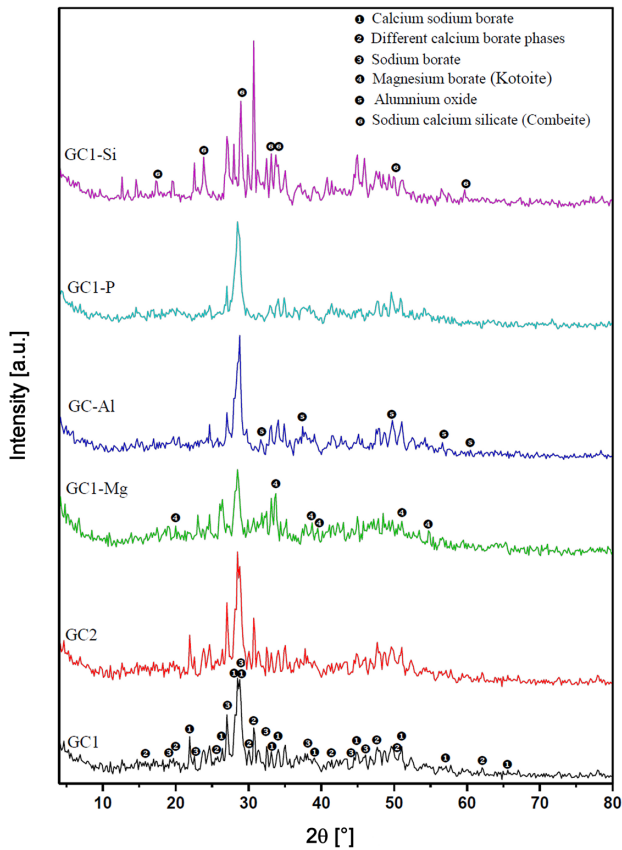


Figure 2. XRD patterns of glass-ceramics derivatives

er [25] have separately identified charge transfer ultra-violet absorption bands in many commercial glasses. They have attributed the presence of such UV spectra to the contamination of unavoidable trace iron impurities within the raw materials used for the preparation of such glasses. Duffy [26] has confirmed such an assumption and has introduced a clear differentiation between charge transfer UV bands due to transition metal ions and other UV bands due to Pb^{2+} and Bi^{3+} ions. Ehrt *et al.* through successive investigations [27,28] have reconfirmed such statements and have concluded that

the presence of iron impurities even at the ppm level could impair the usefulness of special optical glasses. Recent work by ElBatal and others have identified the strong charge transfer UV bands in lithium borate and sodium borate glasses [29,30] and have concluded that such UV absorption originates from trace iron impurities within the materials used for the preparation of such borate glasses.

3.2 X-ray diffraction analysis

Figure 2 shows the X-ray diffraction patterns of the prepared glass-ceramics from the heat treatment of the parent glasses. The obtained phases are listed and summarized in Table 3.

The examination of the crystalline phases which are formed during controlled heat treatments and transformation to corresponding glass-ceramic derivatives shows the presence of calcium sodium borate ($CaO \cdot 3Na_2O \cdot 5B_2O_3$) phase as a main constituent with high intensity (crystallinity) and extended diffraction patterns of all the prepared glass-ceramics.

3.3 FTIR results of glasses and glass-ceramics

Figure 3 presents the FTIR absorption spectra of the prepared glasses before immersion in diluted sodium phosphate solution. The FTIR spectrum of the base glass (G1) shows three very weak absorption kinks at about 490, 520 and 560 cm^{-1} followed by a sharp peak of medium intensity at about 700 cm^{-1} and broad intense band centered at about 1020 and 1420 cm^{-1} with a kink at about 1230 cm^{-1} on the ascending lobe. Small kink and successive peaks at about 2300, 2850, 2920 and 3100 cm^{-1} were also observed. The spectra of the glass G2 shows the same FTIR spectral bands for the sample G1 but with slightly lower intensities with the increase of B_2O_3 content (or the decrease of the modifier content) in the two soda lime borate glasses. It is obvious that the spectra of these two glasses are very similar indicating the appearance of the same IR bands with the same wavenumber and position.

Table 3: Obtained phases from x-ray diffraction of prepared glass ceramics

	GC1, GC2	GC1-Mg	GC1-Al	GC1-P	GC1-Si
Calcium sodium borate ($CaO \cdot 3Na_2O \cdot 5B_2O_3, 2CaO \cdot Na_2O \cdot 5B_2O_3$)	x	x	x	x	x
Different calcium borate phases ($2CaO \cdot B_2O_3, CaO \cdot B_2O_3, CaO \cdot 2B_2O_3$)	x	x	x	x	
Sodium borate ($Na_2O \cdot 4B_2O_3$)	x	x	x		
Magnesium borate (Kotoite) ($3MgO \cdot B_2O_3$)		x			
Aluminium oxide Al_2O_3			x		
Sodium calcium silicate (Combite) ($2Na_2O \cdot 4CaO \cdot 6SiO_2$)					x

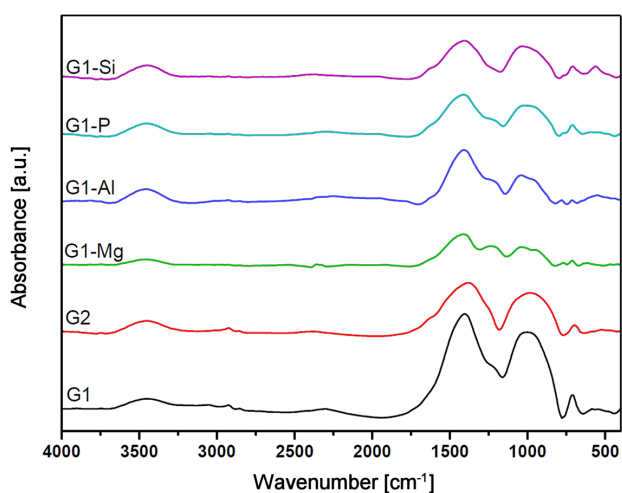


Figure 3 FTIR spectra of studied glasses before immersion

Figure 3 also shows the FTIR spectra of the samples containing 5 wt.% MgO, Al₂O₃, SiO₂ or P₂O₅. It is evident that the FTIR spectra of those samples reveal some small changes either by introducing additional structural groups or show some variations in the bands due to the three-coordinated or four-coordinated boron-oxygen groups.

The spectra appear complex due to the observation of numerous bands extending all over the entire IR regions 400–4000 cm⁻¹. The vibrational modes of the borate network observed in the pure borate glasses are mainly active in three IR spectra regions: 1200–1500 cm⁻¹ (B-O stretching of trigonal BO₃ units), 850–1200 cm⁻¹ (B-O stretching of tetrahedral BO₄⁻ units) and 600–800 cm⁻¹ (bending vibrations of various borate segments) [31,32]. These rich features are based on the fact that boron has the smallest size in comparison to other network forming cations and thus the main vibrational modes associated with borate glass network appear well above 500 cm⁻¹ in the mid-infrared [31,32]. Also, it is evident that the spectrum reveals some of the vibrational sites active in the far-infrared, i.e. 600–400 cm⁻¹ (beginning of measurements), and the near-infrared vibrational modes which include the OH, water and B-OH vibrations.

It is important to mention that the studied glasses contain borate groups as the sole network building units in the three borate glasses (G1, G2 and G1-Mg) and other glass forming groups (e.g. PO₄ and SiO₄) in the sample (G1-Si and G1-P). The following interpretation of all the FTIR spectra takes into consideration the concept adopted by Tarte [33] and Condrate [34] about the free independent vibrations of various structural groups irrespective of the presence of other vibrating groups. This concept is successively applied with glasses containing different structural groups by Dimiriev *et al.* [35,36] and ElBatal *et al.* [37,38]. Also it is born in mind the detailed pub-

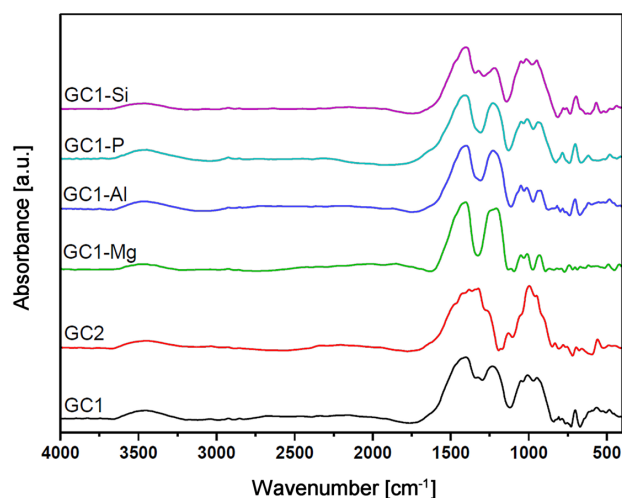


Figure 4. Macrostructure of biogenic HA/glass composite after secondary sintering

lished infrared spectra of borate and phosphate glasses [31,38–41]. The infrared absorption spectra of the studied borate glasses are complex due to the expected appearance of borate groups with different coordinations, (the samples G1 and G2) besides the sharing of some other vibrations due to groups such as PO₄, SiO₄, AlO₄ and MgO₄ in the glasses G1-Mg, G1-Al, G1-Si and G1-P. The medium peak at about 700 cm⁻¹ which is indicative of the bending vibrations or deformation modes of various borate units while the broad intense band at about 1020 cm⁻¹ is referring to the presence of asymmetric stretching vibrations of tetrahedral borate (BO₄⁻) units.

The small peaks observed in the far-infrared region at about 490, 520 and 560 cm⁻¹ are correlated with modifier cations (Na⁺, Ca²⁺) in different residing sites as bridging and nonbridging type [32,41] and the rest of the IR peaks extending from 2850, 2920, 3100 and 3430 cm⁻¹ are correlated with hydrogen bending and molecular water vibrations.

The effects of changing the ratios of B₂O₃, Na₂O, CaO in the glasses (G1, G2) cause no measurable effects on the IR bands indicating the persistence of the main triangular and tetrahedral borate units which are usually identified in borate glasses. The only minor change is the very small variations in the intensities of the IR bands.

Figure 4 illustrates the FTIR spectra of the crystalline glass-ceramic derivatives prepared through controlled crystallization of the parent glasses. The FTIR spectra appear complex and very sharp especially in the mid-region between 800–1500 cm⁻¹ which comprises the distinct vibrational modes due to triangular and tetrahedral borate groups within the studied range of composition. The overall spectral features appear in general as that obtained from the parent glasses, but with distinct appearance of the bands of crystalline materials.

3.4 FTIR results after immersion in liquids

Hench [2] reported that the bioactive silicate glasses and glass-ceramics can be bonded to the bone by the formation of a hydroxyl-carbonate-calcium phosphate (apatite) layer. The formation of this layer on the surfaces of bioactive glasses was shown to occur in fine stages including the ionic exchange process, the formation of silanol (SiOH) layer at the surface, the condensation or depolymerization of SiO₂ rich layer, the migration of Ca²⁺ and PO₄³⁻ groups to form amorphous calcium phosphate layer and finally the crystallization of this layer to HCA layer. Extensive recent studies by Day, *et al.* [17–19] have shown that some borate glasses are readily converted to hydroxyapatite completely and with faster rate than silicate bioglasses and are found to be bioactive in some in vivo experiments [42].

Glasses after immersion in water and Na₂HPO₄

Figures 5 and 6 illustrate the FTIR spectra of the glasses after two methods of immersion. In the first method, the immersion is at 90 °C for 1 hour in distilled wa-

ter and the second is the immersion for 30 days at 37 °C in diluted sodium phosphate solution. In addition, FTIR peak assignment before and after immersion were summarized in Table 4.

Figure 5 shows the FTIR spectra of the glasses after the first method of immersion (90 °C for 1 hour in distilled water). The spectrum of the glass G1 reveals a small peak at about 480 cm⁻¹, two split bands at about 560 and 620 cm⁻¹, a small split peak at about 730 and 770 cm⁻¹ and a very sharp prominent band at about 1000 cm⁻¹ with two medium intensity bands at about 1460 and 1640 cm⁻¹ followed by two small kinks at 2350 and 2580 cm⁻¹ and with final intense broad band centered at about 3450 cm⁻¹. The second borate glass G2 shows the same FTIR spectral characteristics but the intensity of the split band at 560 and 620 cm⁻¹ is lower. The glasses containing Al₂O₃, SiO₂ or P₂O₅ (G1-Al, G1-Si and G1-P) reveal the same FTIR spectral characteristics as the pure borate glasses, but the glass G1-Mg, containing MgO, did not show clearly the split medium intensity band with two peaks.

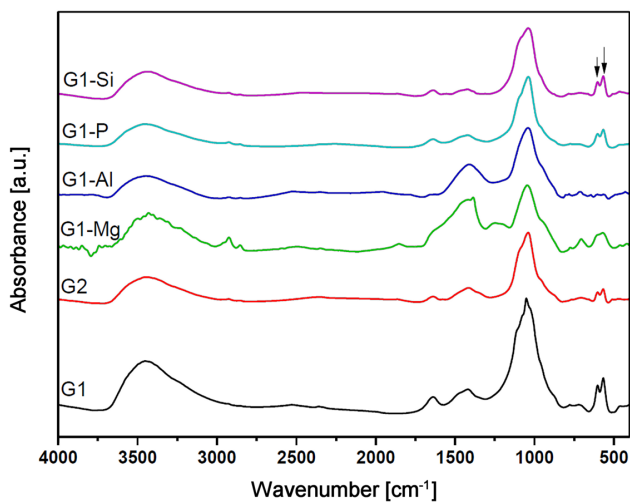


Figure 5. FTIR spectra of glasses after immersion in water at 90 °C for 1 h

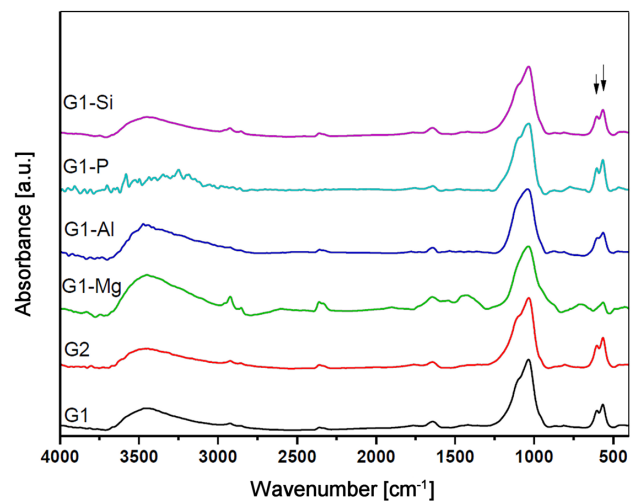


Figure 6. FTIR spectra of glasses after immersion in Na₂HPO₄ for 30 days at 37 °C

Table 4. Infrared absorption bands observed in the borate glasses before immersion, their assignment and related references

Peak position [cm ⁻¹]	Assignment	References
490, 520, 560	Vibrations of metal cations	15, 30–33, 43
625–700	Oxygen bridges between one tetragonal and one trigonal boron atoms	15, 30–33, 43
800–850	Tri-, penta-, diborate groups	15, 30–33, 43
1020–1040	Tri-, penta-, tetraborate, diborate	15, 30–33, 43
1230	Tri-, penta-, tetraborate boroxal groups	15, 30–33, 43
1420–1460	B-O vibrations of various borate groups	15, 30–33, 43
1643	B-O bonds	15, 30–33, 43
2810, 2920, 3100	Hydrogen bonding, water vibrations	15, 30–33, 43
3430–3450	Molecular water	15, 30–33, 43
New vibrations after immersion in phosphate solution for glasses and glass-ceramic derivatives		
566	P-O bonding (crystalline)	2, 15, 19
603	P-O bending (crystalline)	2, 15, 19

Figure 6 shows the FTIR spectra of the glasses after the second method of immersion (30 days at 37 °C in diluted phosphate solution). Inspection of all the spectral curves indicates complete similarity of all the IR bands except the sample G1-Mg which does not have the characteristic split band with two peaks at about 560 and 620 cm^{-1} .

The studied pure borate glasses show the appearance of the two peaks at about 540–565 and 610–660 cm^{-1} after immersion, which are the characteristic indication of apatite crystals [43]. The same statement can hold true for the glasses containing SiO_2 , P_2O_5 and Al_2O_3 . The sample containing MgO did not resolve these peaks after immersion in phosphate solution and thus can be considered to be non-bioactive. This behaviour is correlated with the corrosion results which indicate that the MgO containing glass is the least dissolved sample. It is thus concluded that the ease of solubility of borate glasses is a decisive factor for the bioactivity potential.

Glass-ceramics after immersion in water and Na_2HPO_4

Figures 7 and 8 illustrate the FTIR spectra of the prepared glass-ceramics after immersion in distilled water at 90 °C for 1 hour and in diluted phosphate solution at 37 °C for 30 days.

The IR results show that the glass-ceramics samples (GC1 and GC2) of the pure borate glass show the spectral characteristics of the parent glasses, but the second glass with higher B_2O_3 exhibits lower intensities of the FTIR peaks than the first glass. The two glass-ceramics containing SiO_2 or P_2O_5 (GC1-Si and GC1-P) reveal almost identical spectral features as the pure borate samples. However, the two glass-ceramics containing Al_2O_3 or MgO (GC1-Al and GC1-Mg) did not give the expected curves as the pure borate glasses especially the split band with two peaks around 560–640 cm^{-1} . Moreover, these two samples show also less corrosion weight loss and the X-ray diffraction of the sample containing P_2O_5

did not show any phosphate phases. This may be due to the formation of solid solution with B_2O_3 and this behaviour needs to be studied further.

3.5 Corrosion weight loss

Table 2 gives the corrosion weight loss data obtained from glass grains (0.3–0.6 mm) of the prepared samples after being exposed to the action of 0.25 M sodium phosphate (Na_2HPO_4) solution for 1 hour at 90 °C. The results show that, for the ternary soda-lime-borate glasses (G1-G2), the corrosion weight loss increases with the increase of B_2O_3 or the decrease of modifier oxide content. The glass with P_2O_5 (G1-P) shows the highest weight loss, while the glass containing MgO (G1-Mg) reveals the least weight loss. In addition, glasses containing Al_2O_3 or SiO_2 show relatively higher durabilities, with the glass containing Al_2O_3 having lower weight loss than the glass containing SiO_2 .

Table 2 also shows the corrosion weight loss by the action of distilled water on the same grains. The data reveals that the corrosive or dissolving action of distilled water is lower than the corresponding effect of sodium phosphate for the two ternary soda-lime-borate glasses. With the introduction of SiO_2 or P_2O_5 , the corrosion by distilled water is lower than that obtained by the action of sodium phosphate solution. In addition, the corrosion of glass containing Al_2O_3 reveals approximately the same values with distilled water as that with sodium phosphate, while with the introduction of MgO, the glass shows higher value with water than with sodium phosphate solution.

It is generally accepted that the corrosion of alkali borate glasses is quite different than the corrosion for alkali silicate glasses. When a glass comes in contact with aqueous solutions, the extent of corrosion depends on several factors including the type and ease of cations release from glass to aqueous solution and the ease of solubility of the released cations into solution. The corrosion is also

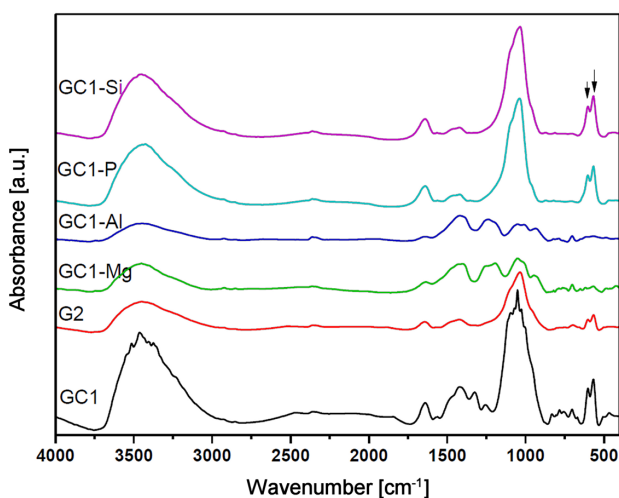


Figure 7. FTIR spectra of glass-ceramic derivatives after immersion in water at 90 °C for 1 h

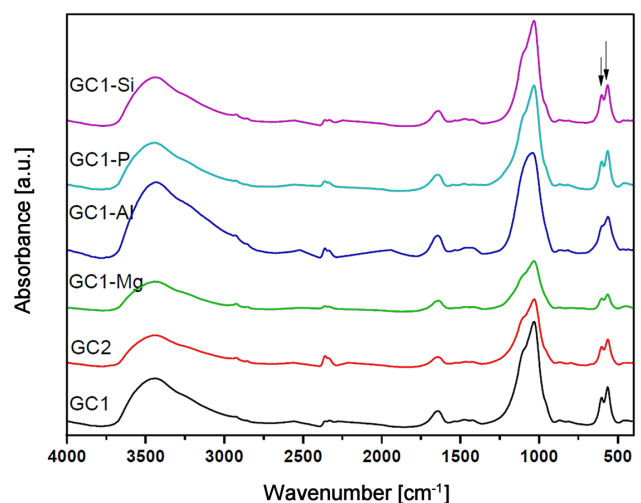


Figure 8. FTIR spectra of glass-ceramic derivatives after immersion in Na_2HPO_4 for 30 days at 37 °C

depending on whether the cations occupy network forming or modifying sites in the glass constitution. When alkali silicate and alkali lime silicate glasses are in contact with aqueous solutions, the corrosion mechanism is accepted to proceed by ion exchange in which modifier cations (alkali or alkaline earth cations) are selectively extracted from glass by attacking solutions [20,23,44,45]. This type of attack is the preferred reaction by water and acidic solutions for silicate glasses. With continuous reaction, the released alkali dissolves and forms alkali hydroxide which disrupts siloxane bonds and parts of the silica network are continuously dissolved with the increase of the pH of the solution.

On the other hand, when alkali borate or alkali alkaline earth borate glasses are exposed to aqueous solutions, almost all of the constituents are attacked and dissolved but to different degrees depending on the nature of both attacking solution and involved cations within the glass, the type of linking within the network and the degrees of the solubility of the constituents in the attacking solution.

The obtained experimental corrosion weight loss data can be understood and explained in accordance with the literature data [20,23,44,45]. The constituent oxides of the first two glasses studied B_2O_3 , Na_2O , CaO are known to dissolve depending on the type of acidic constituents. B_2O_3 is highly soluble in water and vitreous B_2O_3 is highly hygroscopic. With the addition of Na_2O and/or CaO the produced glasses are quite resistant to the immediate action of water because the looser triangular borons are transformed to the compact tetrahedral borons which did not only noticeably increase the durability but also increase the transformation and softening temperatures. This structural variation explains the observed results of the corrosion in the three soda-lime-borate glasses by a sodium phosphate solution.

The introduction of 5 wt.% of SiO_2 , Al_2O_3 or MgO in the host soda-lime-borate glass is observed to increase the durability as expressed by the lower weight loss data. This can be explained by the introduction of extra structural building groups (SiO_4 , AlO_4 or MgO_4) which can strengthen the network structure and makes the corrosion process difficult. The difference between these oxides comes from the possibility of forming insoluble $Al(OH)_3$ with the attacking ionized leaching sodium phosphate solution, which retards the corrosion process. The same assumption seems to hold for $Mg(OH)_2$ besides the interfering effect of Mg^{2+} ions when some of these ions in modifying or bridging sites blocks the passage of other modifier cations in the percolation pathway channels proposed by Greaves [46] during the corrosion process.

The traditional method of measuring chemical durability of glasses has been to estimate the weight change of glass grains or powders after treatment with the corroding solution [20,21,23]. Weight change provides an

easy and rapid method for measuring dissolution process of glasses. The procedure adopted in this work which comprises of leaching large surface area grains at 90 °C for 1 hour. This procedure is assumed by Bacon [47] to be equivalent to the action of the leaching solution on glasses extended to about 1 year at room temperature.

The leaching process by sodium phosphate solution (0.25 M) is observed to be somewhat stronger as a leaching agent and this behaviour may be combined with ionization [23] of sodium phosphate (Na_2HPO_4) salt in aqueous solution to both strong basic and acidic components, namely $2Na^+$ and HPO_4^{2-} . These two components are expected to be corrosive towards the glasses and all their constituents. This behaviour may be discussed in terms of the corrosive nature of sodium phosphate solution and the ionized species of phosphoric acid (HPO_4) to different materials. Parry [48] found that the sodium phosphate solution is more corrosive towards optical glasses containing lanthanum and lead than caustic soda solution. Becker [49] assumed that the reduced state of phosphoric acid could be responsible for the high corrosion rates of stainless steel. Greenfield and Clift [50] recommended that the phosphoric acid should not be stored for a long time in glass bottles because it attacks both silica and alkali. All the previous three results support our assumption that sodium phosphate solution is recommended for the testing of biomaterials.

IV. Conclusions

Two soda-lime-borate glasses together with samples containing substituted 5 wt.% of any of SiO_2 , Al_2O_3 , P_2O_5 or MgO instead of B_2O_3 were prepared. Dissolution behaviour of (0.3–0.6 mm) grains of the samples immersed in 0.25 M sodium phosphate (Na_2HPO_4) solution at 90 °C for 1 h were calculated together with the effect of distilled water. The samples were converted to their glass-ceramic derivatives by controlled heat treatment. The crystallized specimens were examined by X-ray diffraction analysis to determine the formed crystalline phases. The same dissolution experiment was repeated on the glass-ceramics derivatives. Fourier-transform infrared spectroscopic measurements were done for the glasses and glass-ceramics derivatives before and after immersion in water and phosphate solution to confirm the formation of hydroxyapatite as an indication of bioactivity. The dissolution data are discussed on the basis of the current views on the corrosion behaviour of the borate glasses and the dependency on the type of the cations inserted and the way they are housed in the structural network, the ease of solubility or formation of insoluble precipitates during the dissolution process. Infrared spectra indicate the formation of the two peaks characteristics for the hydroxyapatite in the pure borate glass and glasses containing SiO_2 , P_2O_5 and Al_2O_3 and hence are an indication of their bioactivity.

References

1. L.L. Hench, R.J. Splinter, W.C. Allen, K.J. Greenlee, "Bonding mechanisms at the interface of ceramic prosthetic materials", *J. Biomed. Mater. Res.*, **2** (1971) 117–141.
2. L.L. Hench, "Bioceramics: From concept to clinic", *J. Am. Ceram. Soc.*, **74** (1991) 1487–1510.
3. H. Bromer, E. Pfell, H.H. Kos, *German Patent*, No. 2.326.100, 1973.
4. T. Kokubo, S. Ito, S. Sakka, T. Yamamuro, "Formation of a high-strength bioactive glass ceramic in the system MgO-CaO-SiO₂-P₂O₅", *J. Mater. Sci.*, **21** (1986) 536–540.
5. M. Akao, H. Aokai, K. Kalo, "Mechanical properties of sintered hydroxyapatite for prosthetic applications", *J. Mater. Sci.*, **16** (1981) 809–812.
6. P. Vincenzini, *Ceramics in Clinical Applications*, Elsevier, Amsterdam, 1987.
7. T. Kokubo, "Bioactive glass ceramics: Properties and applications", *Biomater.*, **12** (1991) 155–163.
8. L.L. Hench, "Bioactive materials; the potential for tissue regeneration", *J. Biomed. Mater. Res.*, **41** (1998) 511–518.
9. P.Y. Shih, S.W. Yung, T.S. Chin, "Thermal and corrosion behavior of P₂O₅-Na₂O-CuO glasses", *J. Non-Crystal. Solids*, **224** (1998) 143–152.
10. V. Salih, K. Franks, M. James, J.M. Hastings, J.C. Knowles, J. Olsen, "Development of soluble glasses for biomedical use. Part II: The biological response of human osteoblast cell lines to phosphate-based soluble glasses", *J. Mater. Sci. Mater. Med.*, **11** (2000) 615–620.
11. T. Kasuga, Y. Hosoi, M. Nogami, M. Minomi, "Apatite formation on calcium phosphate invert glasses in simulated body fluid", *J. Am. Ceram. Soc.*, **84** (2001) 450–452.
12. F.H. El-Batal, E.M.A. Khalil, Y.M. Hamdy, H.M. Zidan, M.S. Aziz, A.M. Abdelghany. "Infrared reflection spectroscopy for precise tracking of corrosion behavior in 3d-transition metals doped binary lead silicate glass", *Physica B*, **504** (2010) 1294–1300.
13. A.M. Abdelghany, "Novel method for early investigation of bioactivity in different borate bioglas", *Spectrochim. Acta A*, DOI:10.1016/j.saa.2012.02.051.
14. A. Osaka, S. Hayakawa, K. Tsuru, C. Ohtsuki, "Bioactivity of alkali and alkaline Earth borosilicate glasses", pp. 490–497 in *Proc. 2nd Inter. Conf. Borate Glasses, Crystals & Melts*. Ed. A.C. Wright, S.A. Feller, A.C. Hannon, The Society of Glass Technology, Sheffield, 1997.
15. F.H. ElBatal, A.A. ElKhashen, "Preparation and characterization of some substituted bioglasses and their ceramic derivatives from the system SiO₂-Na₂O-CaO-P₂O₅ and effect of gamma irradiation", *Mater. Chem. Phys.*, **110** (2008) 352–362.
16. M.N.C. Richard, *Bioactive behavior of a borate glass*, MS Thesis, University of Missouri-Rolla, 2000.
17. W. Huang, M.N. Rahman, D.E. Day, Y. Li, "Mechanisms for converting bioactive silicate, borate, and borosilicate glasses to hydroxyapatite in dilute phosphate solution", *Phys. Chem. Glasses: Eur. J. Glass Sci. Technol. B*, **47** (2006) 647–658.
18. Q. Wang, W. Huang, D.E. Day, K. Kittratanapiboon, M.N. Rahman, "Preparation of hollow hydroxyapatite microspheres", *J. Mater. Sci. Mater. Med.*, **17** (2006) 583–596.
19. S.B. Jung, D.E. Day, "Conversion kinetics of silicate, borosilicate, and borate bioactive glasses to hydroxyapatite", *Phys. Chem. Glasses: Eur. J. Glass Sci. Technol. B*, **50** [2] (2009) 85–88.
20. R.G. Newton, "Durability of glass. A review", *Glass Technol.*, **26** (1985) 21–38.
21. ISO-standard 6872 Dental Ceramics, 1995 (E)6.
22. I. Szabo, G. Nagy, G. Volksch, W. Holland, "Structure, chemical durability and microhardness of glass-ceramics containing apatite and leucite crystals", *J. Non-Cryst. Solids*, **272** (2000) 191–199.
23. A.M. Abdelghany, H.A. ElBatal, F.M. EzzElDin, "Bone bonding ability behavior of some ternary borate glasses by immersion in sodium phosphate solution", *Ceram. Int.*, **38** (2012) 1105–1113.
24. F.H. ElBatal, M.A. Azooz, Y.M. Hamdy, "Preparation and characterization of some multicomponent silicate glasses and their glass-ceramics derivatives for dental applications", *Ceram. Int.*, **35** (2009) 1211–1218.
25. L. Cook, K.H. Mader, "Ultraviolet transmission characteristics of a fluorophosphate laser glass", *J. Am. Ceram. Soc.*, **65** (1982) 597–601.
26. J.A. Duffy, "Charge transfer spectra of metal ions in glass", *Phys. Chem. Glasses*, **38** (1997) 289–294.
27. U. Natura, D. Ehrt, "Formation of radiation defects in silicate and borosilicate glasses caused by UV lamp and excimer laser irradiation", *Glustech. Ber. Glass Sci. Technol.*, **72** (1999) 295–301.
28. D. Moncke, D. Ehrt, "Irradiation induced defects in glasses resulting in the photoionization of polyvalent dopants", *Optoelectr. Mater.*, **25** (2004) 425–437.
29. F.H. ElBatal, A.A. ElKhashen, M.A. Azooz, S.M. Abo-Naf, "Gamma ray interaction with lithium diborate glasses containing transition metals ions", *Optoelectr. Mater.*, **30** (2008) 881–841.
30. M.A. Ouis, A.M. Abdelghany, H.A. ElBatal, "Corrosion mechanism and bioactivity of borate glasses analogue to Hench's bioglass", *Process. Applic. Ceram.*, **6** [3] (2012) 141–149.
31. E.I. Kamitsos, A.P. Patsis, M.A. Karakassides, G.D. Chryssikos, "Infrared reflectance spectra of lithium borate glasses", *J. Non-Cryst. Solids*, **126** (1990) 52–67.
32. E.I. Kamitsos, "Infrared studies of borate glasses", *Phys. Chem. Glasses*, **44** (2003) 79–87.
33. P. Tarte, "Identification of Li-O bands in the infra-red spectra of simple lithium compounds containing LiO₄ tetrahedra", *Spectrochim. Acta*, **20** (1964) 238–240.
34. R. Condrate, p. 101 in *Introduction to Glass Science*, Plenum Press, New York, 1972.

35. Y.B. Dimitriev, V.T. Mihailova, “Glass formation in binary systems with Bi₂O₃ and PbO participation”, *J. Mater. Sci. Lett.*, **9** (1990) 1251–1254.
36. E.M. Gattef, V.V. Dimitrov, Y.M. Dimitriev, A.C. Wright, “A structural study of Bi₂O₃-B₂O₃ glasses”, pp. 112–119 in *Proc. 2nd Inter. Conf. Borate Glasses, Crystals & Melts*. Ed. A.C. Wright, S.A., Feller, A.C. Hannon, The Society of Glass Technology, Sheffield, 1997.
37. F.H. ElBatal, S.Y. Marzouk, “Interactions of gamma rays with tungsten-doped lead phosphate glasses”, *J. Mater. Sci.*, **44** (2009) 3061–3071.
38. F.H. ElBatal, Y.M. Hamdy, S.Y. Marzouk, “UV-visible and infrared absorption spectra of transition metals-doped lead phosphate glasses and the effect of gamma irradiation”, *J. Non-Cryst. Solids*, **355** (2009) 2439–2447.
39. Y.M. Moustafa, K. El-Egili, “Infrared spectra of sodium phosphate glasses”, *J. Non-Cryst. Solids*, **240** (1998) 144–153.
40. R.K. Brow, C.A. Clik, T.M. Alam, “Modifier coordination and phosphate glass networks”, *J. Non-Cryst. Solids*, **274** (2000) 9–16.
41. A.M. Abdelghany, “The elusive role of low level doping transition metal in lead silicate glass”, *Silicon*, **2** [3] (2010) 179–184.
42. Y. Gu, W. Xiao, L. Lu, W. Huang, M.N. Rahman, D. Wang, “Kinetics and mechanisms of converting bioactive borate glasses to hydroxyapatite in aqueous phosphate solution”, *J. Mater. Sci.*, **46** (2011) 47–54.
43. B.O. Fowler, “Infrared studies of apatites. I. Vibrational assignments for calcium, strontium, and barium hydroxyapatites utilizing isotopic substitution”, *Inorg. Chem.*, **13** (1974) 194–207.
44. D.E. Clark, C.G. Pantano, L.L. Hench, *Magazine for Industry*, New York, 1979.
45. A. Paul, *Chemistry of Glasses*, Second Edition Chapman and Hall, New York, 1990.
46. G.N. Greaves, “EXAFS and the structure of glass”, *J. Non-Cryst. Solids*, **71** (1985) 203–217.
47. F.R. Bacon, “The chemical durability of silicate glass - Part one”, *Glass Industry*, **49** (1968) 438–446.
48. R.J. Parry, pp. 264–247 in *The Chemical and Environmental Stability of Optical Glass*, Ed. B. Zaitos, A.E. Clark, G. Pantano, Noyes Publications, New Jersey, 1992.
49. P. Becker, *Phosphates and Phosphoric Acid*, Second Edition, Marcel Dekker, Inc. New York, 1989.
50. S. Greenfield, M. Clift, p. 185 in *Analytical Chemistry of the Condensed Phosphates*, Pergamon Press, Oxford, 1975.